Li et al. *Zool. Res.* 2024, 45(1): 176−188
https://doi.org/10.24272/j.issn.2095-8137.2023.032

ZR | Zoological Research

Article Open Access

Endogenous biosynthesis of docosahexaenoic acid (DHA) regulates fish oocyte maturation by promoting pregnenolone production

Yi Li[1,2], Xuehui Li[1,2], Ding Ye[1,2], Ru Zhang[1,2], Chengjie Liu[1,2], Mudan He[1,2], Houpeng Wang[1,2], Wei Hu[1,2,3], Yonghua Sun[1,2,3,*]

[1] *State Key Laboratory of Freshwater Ecology and Biotechnology*, *Institute of Hydrobiology*, *Innovation Academy for Seed Design*, *Chinese Academy of Sciences*, *Wuhan*, *Hubei* 430072, *China*

[2] *College of Advanced Agricultural Sciences*, *University of Chinese Academy of Sciences*, *Beijing* 100049, *China*

[3] *Hubei Hongshan Laboratory*, *Wuhan*, *Hubei* 430070, *China*

ABSTRACT

Omega-3 polyunsaturated fatty acids (n-3 PUFAs), particularly docosahexaenoic acid (22:6n-3, DHA), play crucial roles in the reproductive health of vertebrates, including humans. Nevertheless, the underlying mechanism related to this phenomenon remains largely unknown. In this study, we employed two zebrafish genetic models, i.e., *elovl2*$^{-/-}$ mutant as an endogenous DHA-deficient model and *fat1* (omega-3 desaturase encoding gene) transgenic zebrafish as an endogenous DHA-rich model, to investigate the effects of DHA on oocyte maturation and quality. Results show that the *elovl2*$^{-/-}$ mutants had much lower fecundity and poorer oocyte quality than the wild-type controls, while the *fat1* zebrafish had higher fecundity and better oocyte quality than wild-type controls. DHA deficiency in *elovl2*$^{-/-}$ embryos led to defects in egg activation, poor microtubule stability, and reduced pregnenolone levels. Further study revealed that DHA promoted pregnenolone synthesis by enhancing transcription of *cyp11a1*, which encodes the cholesterol side-chain cleavage enzyme, thereby stabilizing microtubule assembly during oogenesis. In turn, the hypothalamic-pituitary-gonadal axis was enhanced by DHA. In conclusion, using two unique genetic models, our findings demonstrate that endogenously synthesized DHA promotes oocyte maturation and quality by promoting pregnenolone production via transcriptional regulation of *cyp11a1*.

Keywords: Docosahexaenoic acid; Oocyte maturation; Oocyte quality; Pregnenolone; Microtubule

INTRODUCTION

Polyunsaturated fatty acids (PUFAs) play essential roles in different biological processes, including neural development (Katakura et al., 2009; Lauritzen et al., 2016) and immune inflammation (Arita et al., 2005; Arita et al., 2007). Among the various PUFAs, omega-3 PUFAs (n-3 PUFAs), especially docosahexaenoic acid (22:6n-3, DHA), are highly beneficial for human health, including the prevention of cardiovascular diseases, fatty liver disease, obesity, and neurodegenerative disorders (Swanson et al., 2012; Zhang et al., 2019a). Therefore, n-3 PUFAs, especially DHA, are considered essential dietary nutrients (Muskiet et al., 2004).

Various studies have suggested that both dietary n-3 PUFAs and DHA exert beneficial effects on animal reproduction and fertility (Li et al., 2004; Vrablik & Watts, 2013; Wathes et al., 2007; Zhu et al., 2019). In humans, supplementation with n-3 PUFAs can delay delivery and reduce the risk of premature birth (Olsen et al., 2019). In mice, diets rich in n-3 PUFAs can prolong the female reproductive lifespan and improve oocyte quality into advanced reproductive age (Nehra et al., 2012). *In vitro* studies also suggest that DHA can promote the proliferation and steroidogenesis of bovine granulosa cells, a steroidogenic cell type found in the ovary (Maillard et al., 2018). Nevertheless, to fully reveal the role and mechanism of n-3 PUFAs and DHA in reproduction, genetic models are essential.

In recent decades, several genetic mutations involving fatty acid desaturase (*fads*) and elongase of very-long-chain fatty acids (*elovl*) have been introduced in mice and *Caenorhabditis elegans*, with subsequent research highlighting the importance of endogenously biosynthesized PUFAs in reproduction

Received: 15 March 2023; Accepted: 08 September 2023; Online: 09 September 2023

Foundation items: This study was supported by the Strategic Priority Research Program of the Chinese Academy of Sciences (Precision Seed Design and Breeding, XDA24010108), National Natural Science Foundation of China (31972780 & 31721005), National Key R&D Program of China (2018YFA0801000), and State Key Laboratory of Freshwater Ecology and Biotechnology (2019FBZ05)

*Corresponding author, E-mail: yhsun@ihb.ac.cn

(Vrablik & Watts, 2013). For example, knockout of *elovl2* and mutation of *fads2* in mice result in male sterility (Stoffel et al., 2008; Zadravec et al., 2011), while depletion of *elovl1* and *elovl2* in *C. elegans* results in an increase in saturated fatty acids, a decrease in PUFAs, and disrupted reproduction (Kniazeva et al., 2003). Nonetheless, the precise regulatory mechanism driven by endogenously synthesized PUFAs remains largely unexplored.

Given their developmental and physiological advantages, such as short reproductive cycle, embryo transparency, and high degree of similarity in reproductive regulatory systems with humans (Hoo et al., 2016; Ye et al., 2019; Zhang et al., 2022), zebrafish have emerged as a promising model for studying reproduction and germ cell biology (MacRae & Peterson, 2015; Ye et al., 2022 Wang et al., 2023) as well as the mechanisms underlying fatty acid biosynthesis and lipid metabolism *in vivo* (Monroig et al., 2018; Xu et al., 2023; Zeituni & Farber, 2016). In our recent work, we established two genetic models based on zebrafish, i.e., *fat1* transgenic zebrafish *Tg(CMV:fat1)* as an endogenous DHA-rich model and zebrafish *elovl2*$^{-/-}$ mutants as a DHA biosynthesis-deficient model (Liu et al., 2020; Pang et al., 2014). These models provide the opportunity to investigate the role and mechanism of DHA in reproduction. Zebrafish studies have shown that maternally expressed *cyp11a1* and zygotically expressed *cyp11a2*, encoding cholesterol side-chain enzymes, are critical for the production of pregnenolone (P5), a microtubule-stabilizing reagent and precursor of all steroid hormones (Hsu et al., 2006b; Wang et al., 2022). However, the transcriptional regulation of *cyp11a1* and *cyp11a2* remains to be elucidated.

In this study, we employed the aforementioned zebrafish models to examine the role of DHA in female reproduction. Results showed that endogenous synthesis of DHA enhanced female fecundity and oocyte maturation, while DHA deficiency in *elovl2*$^{-/-}$ females resulted in egg activation defects and impaired microtubule assembly. Mechanistically, endogenously synthesized DHA promoted the transcription of *cyp11a1*, which encodes a cholesterol side-chain enzyme for P5 production, thereby stabilizing microtubule networks in oocytes and promoting egg quality. In conclusion, using the two unique genetic models, our results suggest that endogenously synthesized DHA promotes oocyte maturation and quality by promoting P5 production via transcriptional regulation of *cyp11a1*.

MATERIALS AND METHODS

Zebrafish strains

The zebrafish strains used in this study, including AB (abbreviated WT), *Tg(CMV:Cel.Fat1,CMV:EGFP)*^{ihb22Tg} (abbreviated *fat1*) (Pang et al., 2014), and *elovl2*$^{-/-ihb332}$ (abbreviated *elovl2*$^{-/-}$) (Liu et al., 2020), were maintained and raised at the China Zebrafish Resource Center of the National Aquatic Biological Resource Center (CZRC/NABRC, Wuhan, China, http://zfish.cn). To obtain *elovl2*$^{-/-}$*/Tg(CMV:fat1)* fish (abbreviated *elovl2*$^{-/-}$*/fat1*), *elovl2*$^{-/-}$ mutants were crossed with *fat1* fish to generate *elovl2*$^{+/-}$*/fat1* fish, which were, in turn, incrossed to generate *elovl2*$^{-/-}$*/fat1* fish. The raising density of zebrafish and embryo staging were determined based on previous research (Ye et al., 2022). All experiments involving zebrafish were performed according to the experimental protocols approved by the Institutional Animal Care and Use Committee of the Institute of Hydrobiology, Chinese Academy of Sciences under protocol IHB2015-006.

Experimental diets and feeding

All zebrafish strains received a daily diet of brine shrimp, known to contain only trace amounts of DHA (Pang et al., 2014). Both WT and *fat1* zebrafish were maintained in the same tank from the fertilized egg stage until they were separated at adulthood for experimental procedures. The *elovl2*$^{-/-}$ adult female zebrafish were supplemented with a DHA-rich diet (Nutriera, China) each day for two weeks before mating to ensure an adequate proportion of female offspring, given the extremely low ratio of female offspring under normal feeding conditions. The subsequent feeding conditions of the *elovl2*$^{-/-}$ embryos were the same as those of the other strains. Throughout the whole experiment, an equal number of zebrafish were kept in each tank, consistent per previous study (Pang et al., 2014).

Morphological analysis of ovaries and oocytes

After anesthetization with MS-222 (Sigma, USA), 6-month post-fertilization WT, *elovl2*$^{-/-}$, *fat1*, and *elovl2*$^{-/-}$*/fat1* adult fish were dissected the day after ovulation. The ovaries were collected and weighed to calculate the gonadosomatic index (GSI; gonad weight/body weight×100%). For embryos, oocyte diameter and chorion elevation distance were measured at 15 minutes post-fertilization (mpf) using ImageJ (v.1.53e). Oocyte diameter was the longest distance in the vertical direction of the animal-vegetal axis. Chorion elevation distance was the longest length of the chorion when fully inflated minus the diameter of the oocyte.

Analysis of follicle composition

Freshly dissected zebrafish ovaries were embedded in optimal cutting temperature (OCT) compound, snap-frozen in liquid nitrogen, cryo-sectioned to generate 10 μm thick slices at 100 μm intervals with a frozen microtome (Thermo HM525, USA). The sections were stained with hematoxylin and eosin (H&E), as described previously (Zhang et al., 2020), then photographed using an Olympus BX53 microscope (Japan). Follicles on the sections were staged according to previously reported criteria (Yang et al., 2017). The number of follicles at different stages was counted for each section, and the proportion of each follicle type was calculated. At least three ovaries were examined and analyzed per group.

Germinal vesicle breakdown (GVBD) assay

Dissected ovaries were washed three times with 1×phosphate-buffered saline (PBS) and transferred to oocyte culture medium consisting of 90% Leibovitz's L-15 medium (Gibco, USA) and 10% fetal bovine serum (BI, Israel) with 100 μg/mL penicillin-streptomycin (Gibco, USA). Follicles at different stages were gently separated with tweezers. Dissociated mature follicles were transferred to a new dish of fresh oocyte culture medium. The GVBD ratio was then assessed as described in previous study (Zhang et al., 2020), with some modifications. In brief, mature oocyte-stage follicles were co-cultured with oocyte culture medium containing 17α-20β-dihydroxy-4pregnen-3-one (DHP, Cayman, USA) at 28°C for 2 h. Follicle translucency predicted GVBD success.

Cortical granule exocytosis (CGE) staining

Eggs were squeezed and activated with water, with embryos then collected at 1 min, 5 min, and 15 min after activation, fixed in 4% paraformaldehyde overnight, and stained with

fluorescent dye-conjugated Maclura pomifera agglutinin (MPA, 50 μg/mL, FL-1341, Vector Laboratories, USA) and phalloidin (66 nmol/L) to display cortical granule exocytosis (He et al., 2022). About 20 embryos were measured per group.

Ooplasmic movement analysis

CellTracker™ CM-DiI Dye (100 pg, C7000, Invitrogen, USA) was microinjected into the yolk of newly fertilized embryos near the vegetal pole according to our recent study (He et al., 2022). To record ooplasmic movement, embryos were mounted in small confocal dishes with 1% agarose. For time-lapse analysis, images were captured every 82 s using an inverted microscope (Leica DMI6000B, Germany) with a 10× objective. At least seven embryos were measured per group.

Mature oocyte-stage follicle acquisition

Dissociated mature oocyte-stage follicles were transferred to a new dish of fresh oocyte culture medium. Hair filaments were made into lockets and fixed on the tips of tweezers. Two lockets were gently slid over the follicle surface until the follicular cell layer was peeled off. The follicles were fixed with 4% paraformaldehyde for subsequent microtubule abundance assay.

Immunofluorescence and microtubule arrangement analysis

Microtubule staining of oocytes and embryos was performed according to previously described procedures (Tran et al., 2012). The antibodies used for immunofluorescence were mouse anti-α-tubulin primary antibody (Invitrogen, 1:500, USA) and Alexa 568 mouse Fluor-conjugated secondary antibody (Invitrogen, 1:500, USA). Microtubule arrangement was assessed according to previous research (Hsu et al., 2006b). For embryos, images were acquired using a laser-scanning confocal inverted microscope (SP8, Leica, Germany). For oocytes, images were acquired using a single molecule confocal microscope (STELLARIS 8, Leica, Germany). ImageJ (v.1.53e) was used to measure α-tubulin fluorescence area per unit area, and relative α-tubulin density was calculated by comparing the experimental group area with that of the control group.

Drug treatments

For P5 (739545, Sigma, USA) treatment, dechorionated embryos were cultured in 0.3×Danieau buffer containing 2 μmol/L P5 from one-cell stage to shield stage. For nocodazole (M1404, Sigma, USA) treatment, mature follicles were cultured in oocyte culture medium containing 1 μg/mL nocodazole for 1 h.

Morpholino and mRNA injection

The morpholino (MO) targeting *cyp11a1* was sourced from Gene Tools, LLC (USA), with the sequence: 5'- CCATC ACACTCTCTCTCTCTACTT-3' (Hsu et al., 2006b). One-cell stage embryos were injected with *cyp11a1* MO at a dose of 7.5 ng per embryo, as described previously (Wei et al., 2014). Approximately 300 embryos were injected per group. The embryos were imaged and analyzed at 10 hours post-fertilization (hpf).

The coding sequence (CDS) of zebrafish *cyp11a1* (GenBank: NM_152953.2) and mouse *gpr120* (GenBank: NM_181748) were amplified by polymerase chain reaction (PCR), then subcloned into the pCS2+ vector, as described previously (He et al., 2020). The mRNA was synthesized using a SP6 *In Vitro* Transcription Kit (mMACHINE; Ambion, USA). Each mRNA was injected into one-cell stage embryos at a dose of 0.5 ng per embryo.

Luciferase assay

The genomic sequences of *cyp11a1* were obtained from a public database (http://asia.ensembl.org) (ENSDARG 00000002347). The Promoter 2.0 website was used to predict possible promoter activity regions of *cyp11a1*. Based on analytical results, we cloned the −6 787 to −5 297 nt and −2 150 to −1 nt region upstream of the "ATG" start codon to generate a *cyp11a1: luciferase* reporter system. The predicted promoter regions (−6 787 to −5 297 nt and −2 150 to −1 nt) were amplified from the zebrafish genomic DNA and sub-cloned into the luciferase reporter vector. A reverse PCR method was used to construct a mutant type of the luciferase reporter vector with appropriate primers (listed in Supplementary Table S1).

For the embryo assay, 50 ng of luciferase reporter plasmid and 5 ng of Renilla control plasmid (pRL-TK, Promega, USA) were mixed and injected into one-cell stage embryos (Lu et al., 2014). For the cell culture assay, 100 ng of luciferase reporter plasmid and 2.5 ng of Renilla control plasmid were mixed and co-transfected into 293T cells with 500 ng of pCS2+ −GPR120 plasmid or pCS2+ control plasmid. The injected embryos were collected at 6 hpf and the transfected cells were collected 24 h after transfection. Embryos and cells were fully lysed and centrifuged at 12 000 ×*g* for 15 seconds at room temperature, and luciferase activity of the supernatants was measured using a dual luciferase reporter system (E1910, Promega, USA) according to previous research (Wei et al., 2014). Each experiment was repeated three times.

Fatty acid analysis

Approximately 60 mature oocytes were used as one sample for fatty acid extraction. Fatty acid was extracted and measured by gas chromatography-mass spectrometry (GC-MS) according to previously described protocols (Liu et al., 2020; Pang et al., 2014). Four biological replicates were established for each group. Data were processed as a percentage of total fatty acid methyl esters.

P5 measurement

In total, 100 fertilized eggs at 15 mpf or 100 embryos at 6 hpf from one female were collected as one sample for P5 measurement. For adults, at least four females were measured individually. Fish were weighed after ovulation and quick-frozen in liquid nitrogen for subsequent assay. P5 was extracted and measured according to previous research (Wang et al., 2022).

Reverse-transcription quantitative PCR (RT-qPCR)

Total RNA was extracted from oocytes, embryos, and ovaries using TRIzol reagent (Invitrogen, USA). For brains, total RNA was extracted using an RNA Prep Pure Micro Kit (TIANGEN, China). RT-qPCR was performed as described previously (Wang et al., 2022). All RT-qPCR gene-specific primers are listed in Supplementary Table S2.

Statistical analysis

All results were expressed as mean±standard deviation (SD). Differences between two groups were analyzed by Student's *t*-test (one-tailed) or multiple *t*-tests-one per row using GraphPad v.8.3.0, with $P<0.05$ considered statistically significant. Statistical significance is represented by asterisks

(*: P<0.05; **: P<0.01; ***: P<0.001). Graphs were drawn using GraphPad Prism v.8.3.0.

RESULTS

Endogenously synthesized DHA positively affects female reproduction

In our previous studies, we established two genetic models, *fat1* zebrafish and *elovl2*$^{-/-}$ mutant zebrafish (Liu et al., 2020; Pang et al., 2014), and showed that DHA was significantly enriched in the *fat1* zebrafish, but extremely reduced in the *elovl2*$^{-/-}$ mutants. In the current study, during routine reproduction, the *fat1* females exhibited significantly higher fecundity than the WT controls, whereas the *elovl2*$^{-/-}$ females exhibited significantly lower fecundity than the WT controls (Figure 1A). Dissection of the ovaries showed that the *fat1* ovaries were significantly larger while the *elovl2*$^{-/-}$ ovaries were much smaller than those from WT siblings (Figure 1B). GSI analysis further confirmed the above results (Figure 1C). Therefore, we examined the fatty acid profiles of oocytes from WT, *fat1*, and *elovl2*$^{-/-}$ mutant zebrafish. Among all fatty acids, only DHA content showed a significant difference among the three groups, i.e., *elovl2*$^{-/-}$ mutant oocytes showed a 0.14-fold decrease (1.2% vs. 8.2%; P<0.001) in DHA content, whereas *fat1* oocytes showed a 1.3-fold increase (10.7% vs. 8.2%; P<0.05) compared to the WT group (Figure 1D). These results suggest that DHA content in oocytes may have a positive effect on reproduction in female zebrafish.

To further analyze the effects of DHA on ovarian follicle development, we performed histological analysis of dissected ovaries and counted the number of follicles at each stage. Results showed that follicle development in ovaries was normal in all groups, with all follicular stages evident. However, the number of vitellogenic and mature follicles was higher in *fat1* ovaries (29.0% vs. 18.8%, P<0.05) compared to WT controls, and the number of early follicles at primary and previtellogenic stages was higher in *elovl2*$^{-/-}$ mutant ovaries (81.2% vs. 71.0%, P<0.05) compared to WT controls (Figure 1E, F), suggesting that follicle differentiation and oocyte maturation were accelerated in *fat1* zebrafish but delayed in *elovl2*$^{-/-}$ mutants. The fertilization rate of *elovl2*$^{-/-}$ oocytes was also much lower than that observed in WT oocytes (Figure 1G, H). These findings suggest that endogenous deficiency of DHA reduces fertility in zebrafish females.

DHA promotes oocyte quality

Oocyte quality is the material basis for oocyte maturation, fertilization, and subsequent embryonic development (Jiao et al., 2023; Miao et al., 2020). The lower fertilization rate and delayed oocyte maturation in *elovl2*$^{-/-}$ mutants suggest that DHA may affect oocyte quality. To confirm this hypothesis, we observed the morphology of oocytes after fertilization. The *fat1* oocytes were relatively brighter, more lustrous, and larger than those of the WT controls (Figure 2A, B), whereas the *elovl2*$^{-/-}$ oocytes were slightly opaque after fertilization. At the one-cell stage, the *elovl2*$^{-/-}$ embryos showed shortened chorion elevation distance compared with WT controls (Figure 2C), indicating that the *fat1* eggs were of better quality while the *elovl2*$^{-/-}$ eggs were of poorer quality. Moreover, *in vitro* GVBD assay indicated that the GVBD proportion was lower in *elovl2*$^{-/-}$ follicles (51.5% vs. 72%, P<0.001) but higher in *fat1* follicles (83.5% vs. 72%, P<0.01) (Figure 2D, E) compared to the WT controls. These results suggest that DHA is essential for oocyte maturation and quality.

Given the reduced fertilization rate in *elovl2*$^{-/-}$ mutants, we next asked whether DHA deficiency could affect egg activation and early embryonic development. To test this hypothesis, cortical granule (CG) exocytosis was assessed in activated eggs by directly visualizing CG content during egg activation (He et al., 2022). At 1 min post-activation (mpa), no significant difference was observed in the CG exocytosis process among the three groups. At 5 mpa, CG exocytosis was almost completed in the *fat1* eggs, but persisted in the WT and *elovl2*$^{-/-}$ eggs. At 15 mpa, the CG exocytosis process was completed in WT eggs, while *elovl2*$^{-/-}$ eggs still retained some CGs (Figure 2F, G). We further tracked ooplasmic motility during early embryonic development and found that motility toward the animal pole was more vigorous in *fat1* embryos, with CellTracker reaching the blastoderm faster than in the WT controls. In contrast, *elovl2*$^{-/-}$ embryos showed sluggish ooplasmic movement, with CellTracker arriving at the blastoderm much slower than in the WT controls (Figure 2H, I; Supplementary Movies S1–S3). These results suggest that DHA promotes ooplasmic movement, egg activation, and early embryonic development.

DHA promotes oocyte quality through production of pregnenolone

As CGs are thought to move along parallel microtubule arrays during egg activation (Tran et al., 2012), and microtubules play an important role in intracellular transport (Akhmanova & Steinmetz, 2015), we speculated whether the role of DHA in oocyte quality is related to microtubule function. As such, we examined the microtubule arrangement in follicles and found that the microtubules were more densely arranged on the surface of *fat1* follicles than in WT controls. When the follicles were treated with the microtubule depolymerization agent nocodazole for 1 h, microtubule arrangement became disordered in all three groups (Figure 3A). The relative a-tubulin intensity was significantly higher in *fat1* follicles than in WT controls (Figure 3B), indicating that microtubule arrangement in *fat1* follicles was more resistant to nocodazole treatment. In contrast, the degree of disordered microtubule arrangement was more severe in *elovl2*$^{-/-}$ follicles. Thus, these observations suggest that microtubule arrangement is less stable in *elovl2*$^{-/-}$ follicles and more stable in *fat1* follicles.

The steroid hormone P5 can stabilize microtubule assembly in zebrafish embryos (Hsu et al., 2006b; Weng et al., 2013). Thus, we wondered whether poor microtubule stability in *elovl2*$^{-/-}$ mutants may be due to low P5 content. After measuring P5 content, we found that the *elovl2*$^{-/-}$ eggs had significantly lower P5 content, while the *fat1* eggs had significantly higher P5 content compared with the WT controls (Figure 3C). We then examined the microtubule structure of the embryos during development. Consistent with previous reports (Hsu et al., 2006b), a large array of microtubules oriented along the animal-vegetal axis on the surface of the embryos (Figure 3D). Compared with WT embryos, the microtubule arrangement was slightly denser in *fat1* embryos, although the difference was not significant (Figure 3E), while the length of aligned microtubules was reduced in the *elovl2*$^{-/-}$ mutants. Accordingly, P5 content was significantly higher in *fat1* embryos and lower in *elovl2*$^{-/-}$ embryos compared to the WT group (Figure 3F). Moreover, after incubation with P5, polymerized tubulin length was significantly increased in the

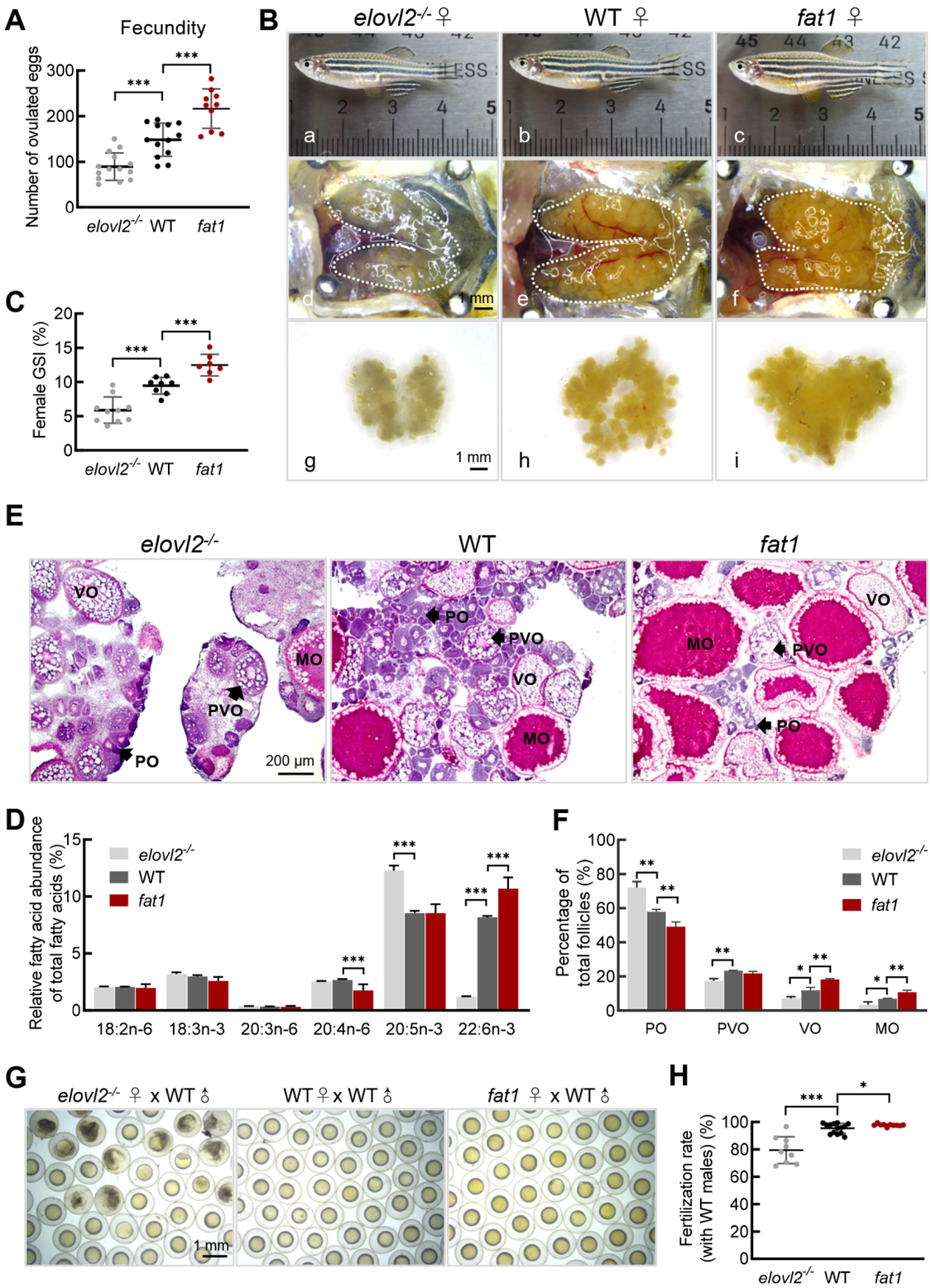

Figure 1 DHA is important for oocyte maturation and successful fertilization

A: Number of eggs laid by WT (*n*=13), *fat1* (*n*=10), and *elovl2*$^{-/-}$ (*n*=14) female zebrafish. B: Morphological and gross anatomical analysis of adult females on day after ovulation at 180 days post-fertilization (dpf). a–c: Morphology of WT, *fat1*, and *elovl2*$^{-/-}$ zebrafish. d–i: Overview of dissected ovaries from WT, *fat1*, and *elovl2*$^{-/-}$ zebrafish. Scale bar: 1 mm. C: GSI of WT (*n*=8), *fat1* (*n*=7), and *elovl2*$^{-/-}$ (*n*=10) zebrafish on day after ovulation. D: Fatty acid composition (molecular percentage) of mature oocytes from WT, *fat1*, and *elovl2*$^{-/-}$, *n*=4. E: H&E staining of WT, *fat1*, and *elovl2*$^{-/-}$ ovaries. Scale bar: 100 μm. F: Follicle quantification of WT, *fat1*, and *elovl2*$^{-/-}$ ovaries on day after ovulation, *n*=3. G: Representative images of embryos from natural mating of WT, *elovl2*$^{-/-}$, and *fat1* females with WT males. Scale bar: 1 mm. H: Comparison of fertilization ratio of groups in panel G. All values are mean±SD. Student's *t*-tests were used in panels A, C, H. Multiple *t*-tests-one per row were used in panels D, F. *: $P<0.05$; **: $P<0.01$; ***: $P<0.001$. Arrows point to follicle cells at different developmental stages. PO: primary oocyte; PVO, previtellogenic oocyte; VO, vitellogenic oocyte; MO, mature oocyte. GSI, gonadosomatic index. H&E, hematoxylin-eosin.

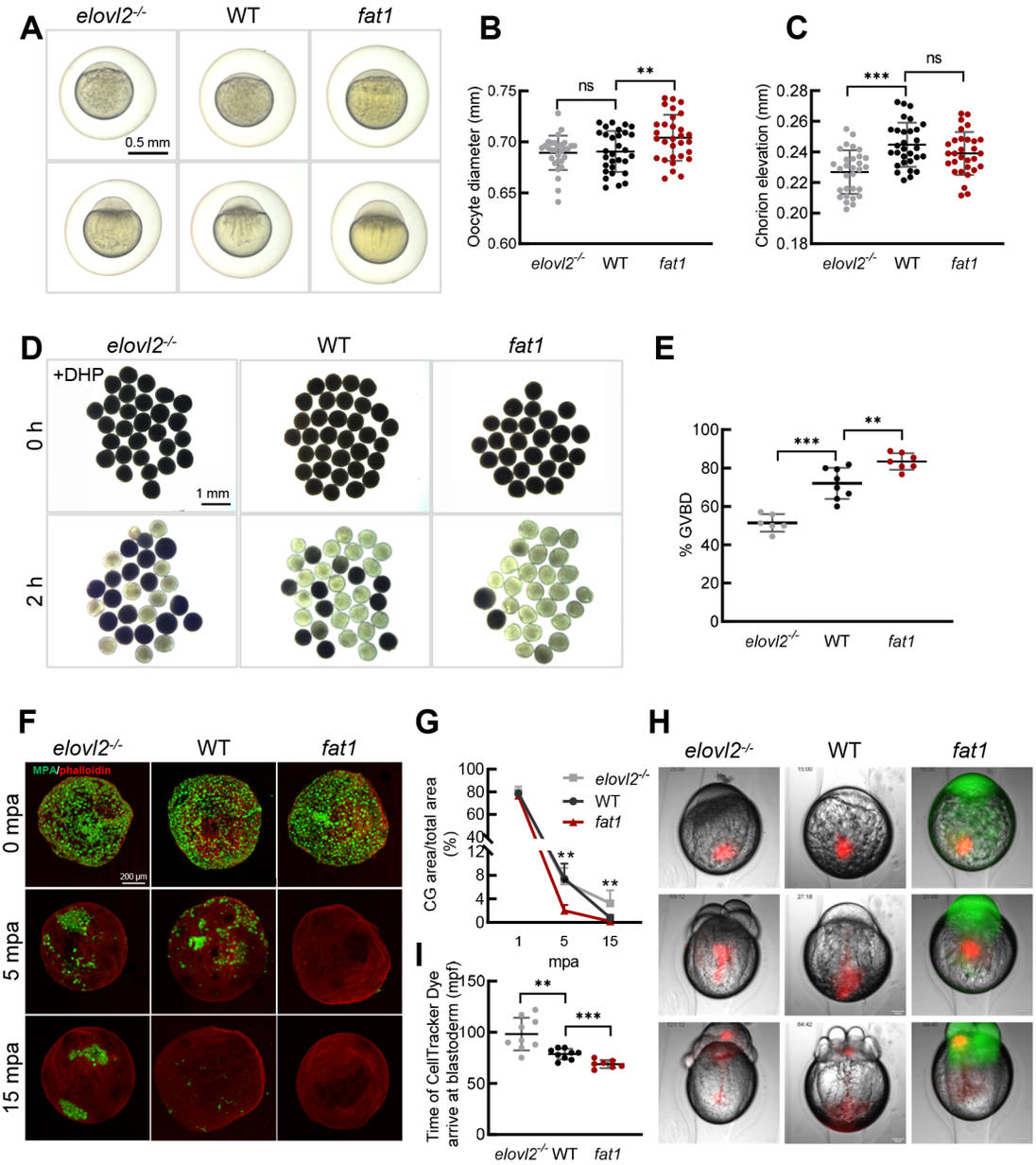

Figure 2 DHA promotes oocyte quality

A: Representative images of WT, *fat1*, and *elovl2*$^{-/-}$ embryos with chorions at 15 and 40 minutes post-fertilization (mpf). Scale bar: 250 μm. B: Measurement of oocyte diameter at 15 mpf. *n*=30. C: Measurement of chorion elevation at 15 mpf. *n*=30. D: Representative images of GVBD assay of WT, *fat1*, and *elovl2*$^{-/-}$ follicles. Scale bar: 1 mm. E: Quantitative results of GVBD assay. F: Maximum z-projection of phalloidin (red) and Maclura pomifera agglutinin (MPA) (green) staining of activated WT, *fat1*, and *elovl2*$^{-/-}$ eggs fixed at 1, 5, and 15 min post-activation (mpa). Scale bar: 50 μm. G: Statistical analysis of total CG positive areas (%) in WT, *fat1*, and *elovl2*$^{-/-}$ eggs. H: Representative images of cytoplasmic movement in WT, *fat1*, and *elovl2*$^{-/-}$ embryos. Images are from time-lapse movies of individual embryos from 15 to 120 mpf injected with CellTracker Dye immediately after fertilization. Scale bar: 100 μm. Number in upper left of image in panel I represents mpf. I: Quantification analysis of cytoplasmic movement in WT, *fat1*, and *elovl2*$^{-/-}$ embryos. Quantification is defined as time of CellTracker Dye arrival in blastoderm. At least seven embryos were measured per group. All values are mean±SD. Student's *t*-tests were used in panels B, C, E, I. Multiple *t*-tests-one per row were used in panels G. ns: No significance; *: P<0.05; **: P<0.01; ***: P<0.001.

elovl2$^{-/-}$ mutant embryos (Figure 3G). Fluorescence intensity analysis further confirmed these rescue effects (Figure 3H). Thus, these results indicate that low P5 content is responsible for the poor microtubule stability in *elovl2*$^{-/-}$ embryos, while sufficient P5 content stabilizes microtubule assembly in *fat1* embryos.

To investigate the mechanism underlying the different P5 levels in the three groups, we first examined the expression of *cyp11a1*, which encodes the cholesterol side-chain cleavage enzyme (Hsu et al., 2009; Hu et al., 2004). Results showed that expression of *cyp11a1* was significantly lower in *elovl2*$^{-/-}$ eggs and embryos, but significantly higher in *fat1* eggs and embryos compared with the WT controls (Figure 3I), suggesting that *cyp11a1* expression may affect P5 content and thus microtubule stability. To confirm this, we knocked down *cyp11a1* expression using a previously validated MO (Hsu et al., 2006b), and carefully compared the phenotypes of 10 hpf embryos injected with low-dose *cyp11a1* MO. After the

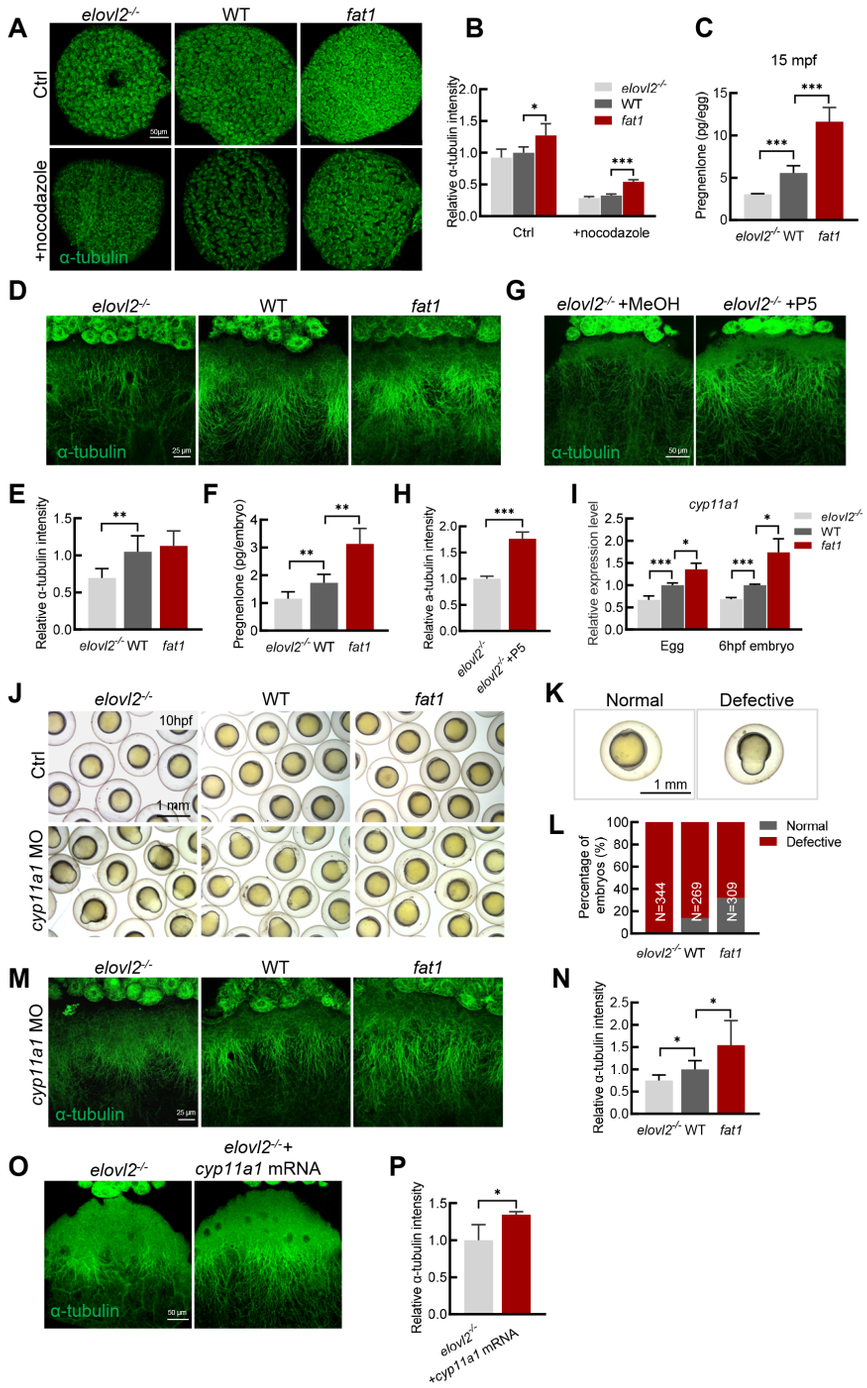

Figure 3 DHA promotes oocyte quality through production of pregnenolone

A: Representative images of anti-α-tubulin staining of mature follicles from WT, *fat1*, and *elovl2*$^{-/-}$ zebrafish treated with methanol (Ctrl) or 1 μg/mL nocodazole. Scale bar: 50 μm. B: Quantification of α-tubulin intensity of groups in panel A. Relative α-tubulin intensity was calculated by comparing fluorescence area of embryos from each experimental group with that of the WT group treated with methanol per unit area. At least three embryos were measured per group. C: Pregnenolone (P5) content in WT, *fat1*, and *elovl2*$^{-/-}$ embryos at 15 mpf. D, E: Representative images and quantitative analysis of anti-α-tubulin staining of WT, *fat1*, and *elovl2*$^{-/-}$ embryos at 6 hpf. Scale bar: 25 μm. At least four embryos were measured per group. F: P5 content in WT, *fat1*, and *elovl2*$^{-/-}$ embryos at 6 hpf. G, H: Representative images and quantitative analysis of anti-α-tubulin staining of *elovl2*$^{-/-}$ embryos incubated with methanol (MeOH, Ctrl) or P5 for 6 hpf. Scale bar: 25 μm. I: Real-time qPCR of *cyp11a1* expression in WT, *fat1*, and *elovl2*$^{-/-}$ eggs and 6 hpf embryos. J–L: Representative images and statistical analysis of WT, *fat1*, and *elovl2*$^{-/-}$ embryos with normal development or knockdown of *cyp11a1* at 10 hpf. Scale bar: 1 mm. Approximately 300 embryos were measured per group. M, N: Representative images and quantitative analysis of anti-α-tubulin staining of *cyp11a1* knockdown embryos at 6 hpf from WT, *fat1*, and *elovl2*$^{-/-}$ zebrafish. Scale bar: 25 μm. At least four embryos were measured per group. O, P: Representative images and quantitative analysis of anti-α-tubulin staining of *elovl2*$^{-/-}$ embryos with normal development or injected with *cyp11a1* mRNA. Scale bar: 25 μm. At least three embryos were measured per group. All values are mean±SD. Student's *t*-tests were used in panels C, E, F, H, L, N, P. Multiple *t*-tests-one per row were used in panels B, I. *: P<0.05; **: P<0.01; ***: P<0.001.

injection, 86% of the WT embryos showed epiboly defects, whereas 100% of *elovl2*$^{-/-}$ embryos and only 68% of *fat1* embryos showed defects (Figure 3J-L). At 36 hpf, although uninjected embryos from the three groups (WT, *elovl2*$^{-/-}$, *fat1*) showed a survival rate of nearly 100% (Supplementary Figure S1A, B), after low-dose *cyp11a1* MO injection, none of the *elovl2*$^{-/-}$ embryos survived, while 41.3% of WT embryos and 58.7% of *fat1* embryos survived (Supplementary Figure S1A, C). These observations suggest that DHA-deficient *elovl2*$^{-/-}$ embryos are more sensitive and DHA-rich *fat1* embryos are more resistant to *cyp11a1* knockdown.

We further examined microtubule arrangement after *cyp11a1* knockdown. Disruption of *cyp11a1* function led to a diminished microtubule arrangement in the embryos of all three groups. However, microtubule density was lower in *elovl2*$^{-/-}$ embryos and much higher in *fat1* embryos compared to the WT controls (Figure 3M, N). After injection of *cyp11a1* mRNA, the density of aligned microtubules was significantly increased in the *elovl2*$^{-/-}$ mutants (Figure 3O). These findings were confirmed by fluorescence intensity analysis (Figure 3P), indicating that microtubule assembly defects in *elovl2*$^{-/-}$ embryos are caused by a deficiency of *cyp11a1* and its catalytic product P5. Overall, our results suggest that DHA can improve oocyte quality through stabilizing microtubule arrangement.

DHA promotes P5 production by regulating *cyp11a1* promoter activity

Next, we investigated whether DHA directly regulates *cyp11a1* transcription. After identification of the active *cyp11a1* promoter region, results showed that the −6 787 to −5 297 nt region exhibited promoter activity (*cyp11a1: luc-2*) (Figure 4A, B). We then explored whether the *cyp11a1* promoter responds to DHA regulation. In HEK293T cells, treatment of 10 nmol/L DHA increased luciferase activity of *cyp11a1: luc-2* when co-transfected with a mammalian DHA receptor GPR120 expression construct (Figure 4C), suggesting that DHA may regulate *cyp11a1* transcription through the G protein-coupled signaling pathway. We further examined *cyp11a1* promoter activity in different groups of zebrafish embryos. At 6 hpf, luciferase activity of *cyp11a1: luc-2* in the *elovl2*$^{-/-}$ mutants was much lower than that observed in WT controls, while incubation with DHA significantly increased luciferase activity both in the *elovl2*$^{-/-}$ mutants and WT controls (Figure 4D), indicating that DHA also regulates *cyp11a1* promoter activity in zebrafish embryos.

DHA is reported to bind to GPR120 to stimulate both protein kinase C (PKC) and mitogen-activated protein (MAP) kinase, ultimately acting on the serum response element (SRE) on the genome to regulate gene expression (Oh et al., 2010). Here, we identified a sequence (TCATATTGGG) on the *cyp11a1* promoter very similar to the inner core 10 nucleotide region (CCATATTAGG) of the SRE. To confirm whether the SRE-like sequence is a DHA responsive domain, we deleted the 210 bp sequence covering the SRE-like region (−5 659 to −5 450 nt) on *cyp11a1: luc-2*. Results showed that luciferase activity of the mutated promoter was significantly decreased in all groups compared to the original promoter (Figure 4E), indicating that this sequence on the *cyp11a1* promoter is the region that responds to DHA regulation. In summary, our findings imply that DHA potentially modulates *cyp11a1* transcription by regulating its promoter activity.

Vertebrate reproduction is controlled by steroid hormones and the conversion of cholesterol to P5 constitutes the initial step in the steroidogenesis pathway (Hsu et al., 2006a; Wang et al., 2022). Given their differences in P5 levels, we further examined the expression of genes associated with steroidogenesis in the three groups. Genes upstream of the hypothalamic-pituitary-gonad (HPG) axis, such as *gnrh3, fshb,* and *lhb*, were up-regulated in *fat1* brains, while related genes, such as *cyp19a1a* and *fshr*, were also up-regulated in *fat1* ovaries after ovulation. In contrast, the expression levels of *lhb* and its receptor (LHR) were down-regulated in *elovl2*$^{-/-}$ brains and ovaries, respectively, compared to the WT controls (Figure 4F, G). Consistently, compared to the WT controls, there was a trend toward increased P5 content in *fat1* fish the day after ovulation (Figure 4H). Overall, these results suggest that the HPG axis is enhanced in DHA-rich *fat1* fish but reduced in DHA-deficient *elovl2* mutant, further amplifying the effects of DHA on oocyte maturation.

***fat1* transgene restores fecundity of *elovl2*$^{-/-}$ mutants**

To further confirm the important role of DHA in oocyte maturation and quality, we crossed the *fat1* transgene into *elovl2*$^{-/-}$ mutant zebrafish to explore potential rescue effects. Analysis of fatty acid composition revealed a significant increase in DHA levels in the *elovl2*$^{-/-}$*/fat1* oocytes compared to the *elovl2*$^{-/-}$ mutants (Supplementary Figure S2). Based on fecundity assessment, *elovl2*$^{-/-}$*/fat1* females exhibited significantly higher fecundity than the *elovl2*$^{-/-}$ mutants (Figure 5A). GSI analysis indicated that *elovl2*$^{-/-}$*/fat1* ovaries were significantly larger than *elovl2*$^{-/-}$ ovaries the day after ovulation (Figure 5B, C). Furthermore, histological analysis demonstrated that the *elovl2*$^{-/-}$*/fat1* ovaries contained more vitellogenic and mature-stage follicles (Figure 5D, E), with a higher proportion of GVBD in the mature follicles, compared to the *elovl2*$^{-/-}$ mutants (Figure 5F, G), suggesting that the *fat1* transgene recovers DHA content in *elovl2*$^{-/-}$ mutants and accelerates oocyte maturation. In addition, *cyp11a1* expression was higher in the *elovl2*$^{-/-}$*/fat1* oocytes than in the *elovl2*$^{-/-}$ oocytes (Figure 5H). Furthermore, after *cyp11a1* knockdown, the *elovl2*$^{-/-}$*/fat1* embryos exhibited fewer epiboly defects and longer microtubule lengths compared to the *elovl2*$^{-/-}$ embryos (Figure 5I-K). Dual-luciferase assay also showed that luciferase activity in all *cyp11a1: luc* reporter types was higher in the *elovl2*$^{-/-}$*/fat1* embryos than in the *elovl2*$^{-/-}$ embryos (Figure 5L). These results highlight the ability of the *fat1* transgene to increase DHA content in *elovl2*$^{-/-}$ embryos and thereby improve *elovl2*$^{-/-}$ oocyte quality, thus supporting the conclusion that DHA plays an important role in oocyte maturation and quality.

DISCUSSION

Previous studies have suggested that dietary supplementation of DHA is beneficial for female reproduction in various vertebrates (Cerri et al., 2009; Chiu et al., 2018; Janati Idrissi et al., 2022; Nehra et al., 2012; Wonnacott et al., 2010). However, how and why DHA promotes oocyte maturation and female reproduction remain unknown. Our study utilized two unique genetic models of zebrafish, *elovl2* mutants deficient in DHA and *fat1* transgenics rich in DHA, to demonstrate the role of endogenously synthesized DHA in proper oocyte maturation and female reproduction. Notably, our results showed that endogenously synthesized DHA promoted oocyte maturation and quality by stimulating progesterone production and activating the HPG axis (Figure 6).

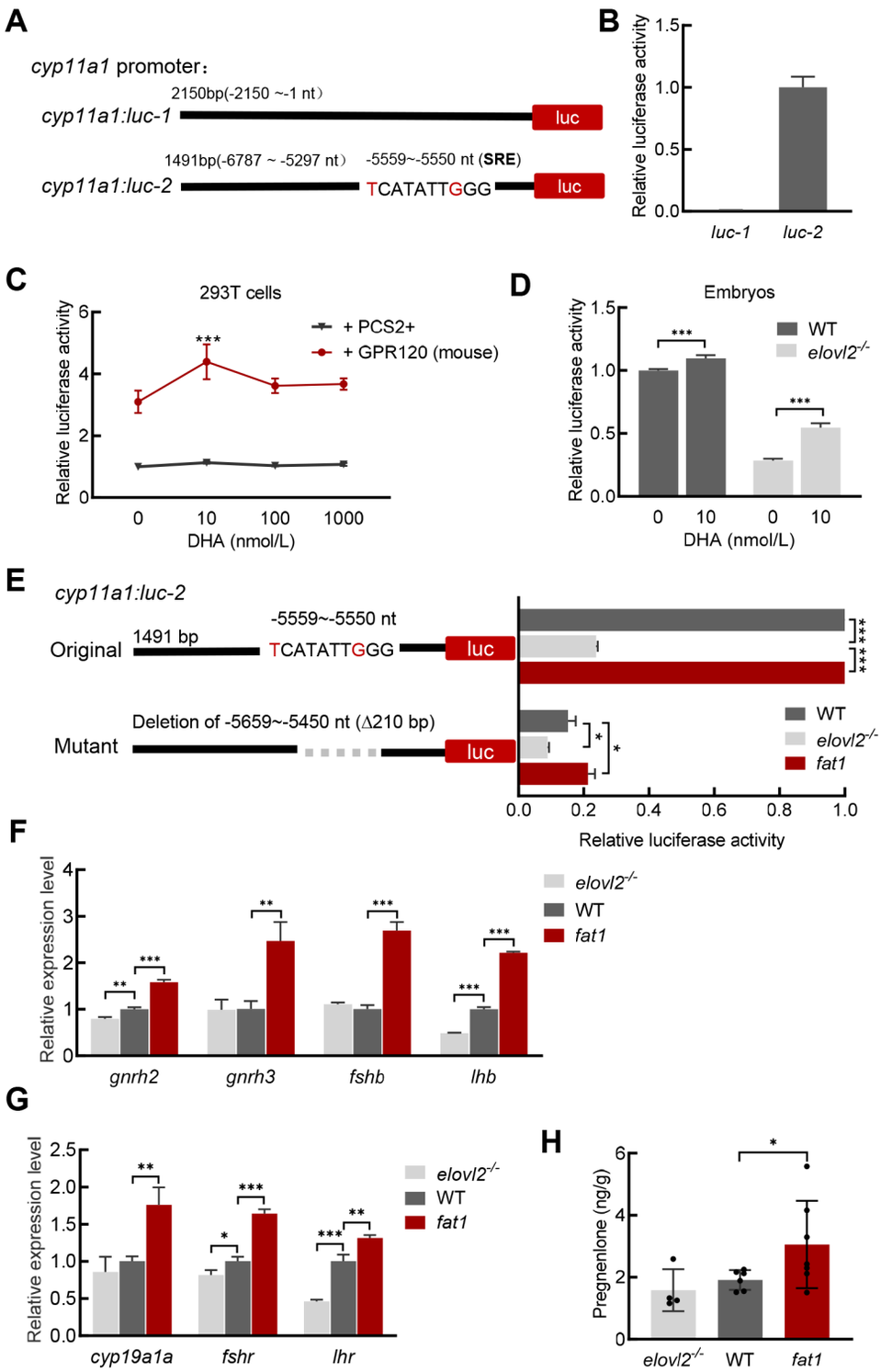

Figure 4 DHA regulates transcription of *cyp11a1* and activates HPG axis

A, B: Schematic of reporter plasmids for *cyp11a1* promoter activity analysis. Luciferase assay showed only *cyp11a1: luc-2* exhibited promoter activity in HEK293T cells. C: Luciferase assay of *cyp11a1* promoter in HEK293T cells. GPR120 increased *cyp11a1* promoter activity and DHA regulated activity of *cyp11a1: luc-2* when co-transfected with GPR120 in HEK293T cells. D: Luciferase assay of *cyp11a1* promoter in WT and *elovl2*$^{-/-}$ embryos at 6 hpf. E: Luciferase assay of different types of *cyp11a1* promoters in WT, *fat1*, and *elovl2*$^{-/-}$ embryos at 6 hpf. F, G: Real-time qPCR of gene expression in HPG axis in brain and gonads of WT, *fat1*, and *elovl2*$^{-/-}$ zebrafish. H: P5 content in WT, *fat1*, and *elovl2*$^{-/-}$ zebrafish females on day after ovulation. At least four fish were measured per group. All values are mean±SD. Student's *t*-tests were used in panels B, D, H. Multiple *t*-tests-one per row were used in panels C, E, F, G. *: $P<0.05$; **: $P<0.01$; ***: $P<0.001$.

Vertebrate reproduction is influenced by many factors, including external factors such as stress (Agarwal et al., 2012) and nutrition (Masoudi et al., 2016), as well as internal factors, such as maternal materials (Gu et al., 2015) and steroids (Krisher, 2013; Ojeda et al., 1979; Zhou, 2013). Previous research using both *in vitro* models and dietary experiments in

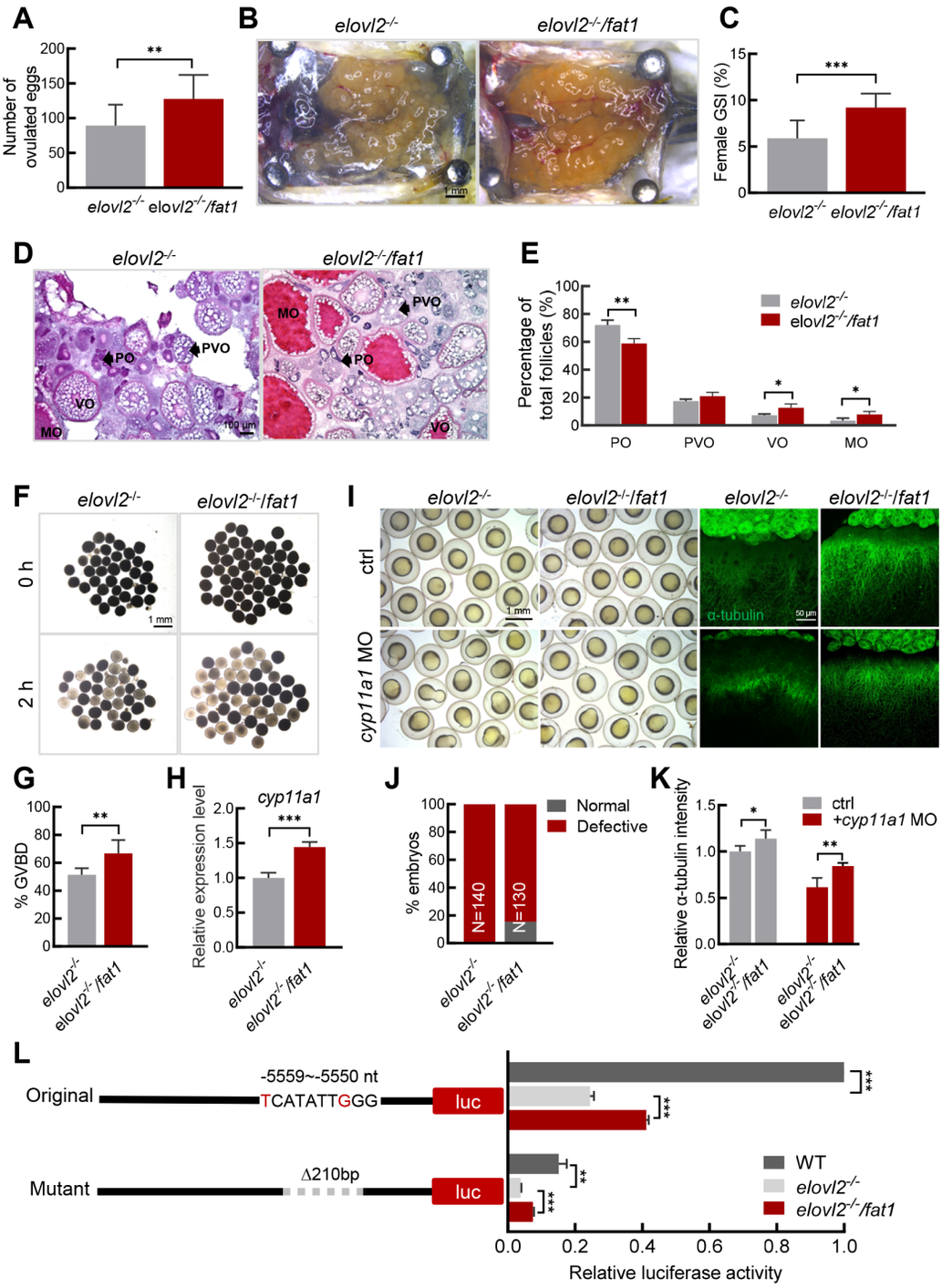

Figure 5 *fat1* transgene restores fecundity of *elovl2*$^{-/-}$ mutant

A: Number of eggs laid by *elovl2*$^{-/-}$ (*n*=14) and *elovl2*$^{-/-}$*/fat1* (*n*=16) female zebrafish. B: Overview of dissected ovaries from *elovl2*$^{-/-}$ and *elovl2*$^{-/-}$*/fat1* zebrafish on day after ovulation at 180 dpf. Scale bar, 1 mm. C: GSI of *elovl2*$^{-/-}$ (*n*=10) and *elovl2*$^{-/-}$*/fat1* (*n*=7) zebrafish on day after ovulation. D: H&E staining of *elovl2*$^{-/-}$ and *elovl2*$^{-/-}$*/fat1* ovaries. Scale bar: 100 μm. E: Follicle quantification of *elovl2*$^{-/-}$ and *elovl2*$^{-/-}$*/fat1* ovaries on day after ovulation. At least three ovaries were measured per group. F, G: Representative images and quantitative results of GVBD assay of *elovl2*$^{-/-}$ and *elovl2*$^{-/-}$*/fat1* follicles. Scale bar: 1 mm. H: Real-time qPCR of *cyp11a1* expression in *elovl2*$^{-/-}$ and *elovl2*$^{-/-}$*/fat1* eggs. I: Representative images of embryo morphology and anti-α-tubulin staining of *elovl2*$^{-/-}$ and *elovl2*$^{-/-}$*/fat1* embryos with normal development or knockdown of *cyp11a1*. J: Statistical analysis of *elovl2*$^{-/-}$ and *elovl2*$^{-/-}$*/fat1* embryo phenotypes with normal development or knockdown of *cyp11a1*. Approximately 130 embryos were measured per group at 10 hpf. K: Quantitative analysis of anti-α-tubulin staining of *elovl2*$^{-/-}$ and *elovl2*$^{-/-}$*/fat1* embryos with normal development or knockdown of *cyp11a1*. At least five embryos per group were measured at 6 hpf. L: Schematic of reporter plasmids for *cyp11a1* promoter activity analysis and luciferase assay of different types of *cyp11a1* promoters in WT, *elovl2*$^{-/-}$, and *elovl2*$^{-/-}$*/fat1* embryos at 6 hpf. All values are mean±SD. Student's *t*-tests were used in panels A, C, G, H, J. Multiple *t*-tests-one per row were used in panel E, K, L. *: P<0.05; **: P<0.01; ***: P<0.001. Arrows indicate follicle cells at different developmental stages. PO: primary oocyte; PVO, previtellogenic oocyte; VO, vitellogenic oocyte; MO, mature oocyte. GSI, gonadosomatic index; H&E, hematoxylin-eosin.

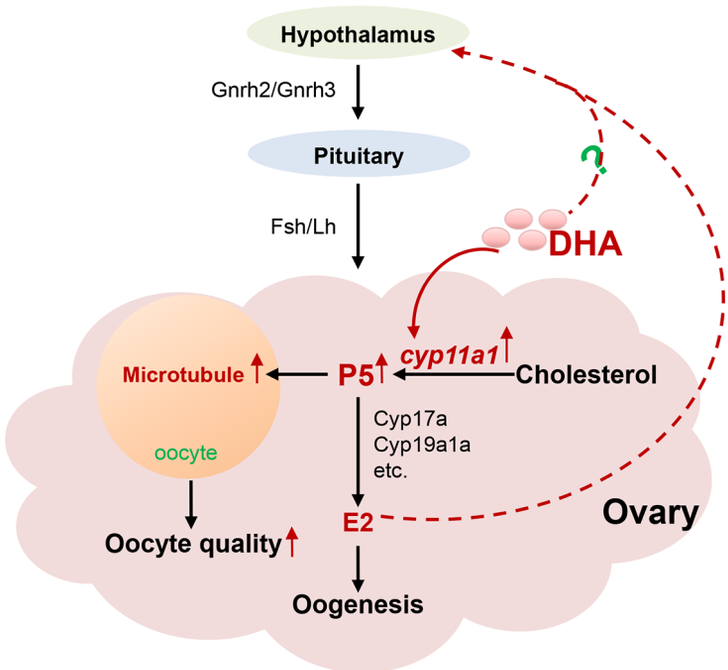

Figure 6 Graphic summary of role of DHA in oocyte maturation and oocyte quality

Endogenously synthesized DHA promotes oocyte maturation and oocyte quality by promoting progesterone production and, in turn, activating the HPG axis.

animals has demonstrated that DHA supplementation can positively regulate reproduction by enhancing HPG axis activation and steroid production (Maillard et al., 2018; Qi et al., 2019; Tocher, 2003; Tran et al., 2016; Wonnacott et al., 2010; Xu et al., 2017). Nevertheless, the underlying mechanism remains poorly elucidated. In the present study, we showed that DHA promoted the synthesis of the precursor of steroid hormones, P5, which, in turn, activated the HPG axis pathway to ensure normal oogenesis. Based on luciferase reporter assays *in vitro*, cultured cells, and *in vivo* embryos, our study further demonstrated that DHA may directly regulate the promoter activity of the *cyp11a1* gene, which encodes the cholesterol side-chain cleavage enzyme (Hsu et al., 2006b; Wang et al., 2022). Cyp11a1 converts cholesterol to P5, which then binds the microtubule plus end-tracking protein, cytoplasmic linker protein 1 (CLIP-170), stabilizing microtubules in early embryos (Hsu et al., 2006b; Weng et al., 2013). In this study, we found that oocyte-originated DHA regulated *cyp11a1* promoter activity during oocyte maturation, thereby promoting oocyte quality. Together with our recent work (Wang et al., 2022), this study reinforces the conclusion that P5 not only promotes early embryonic development but also promotes oocyte development and maturation. Given the recent generation of *fat1* transgenic common carp (*Cyprinus carpio*) (Zhang et al., 2019b), analyzing reproduction and oocyte quality in DHA-rich common carp would be of interest.

DHA has been implicated in the maintenance of spindle shape and size and microtubule morphology stability in vertebrate oocytes during meiosis (Nehra et al., 2012). In addition, DHA is reported to protect neural structural plasticity by prevention of tubulin loss (Loehfelm et al., 2020; Pusceddu et al., 2016; Serrano-García et al., 2018). These observations suggest that DHA plays an important role in stabilizing microtubule structure. The dynamic assembly of microtubules in the yolk is also critical for normal embryonic development in fish (Jesuthasan & Strähle, 1997; Sun et al., 2001; Tran et al., 2012). Our findings indicated that DHA enhances microtubule assembly stability through the up-regulation of *cyp11a1* transcription and P5 synthesis, both pivotal during oogenesis and early embryonic development.

In vitro and *in vivo* experiments have shown that DHA can mediate intracellular signaling in mammals via the G protein-coupled receptor GPR120 (Han et al., 2018; Hilgendorf et al., 2019; Hirasawa et al., 2005; Shin et al., 2019). DHA can bind GPR120 to stimulate PKC and MAP kinase, eventually acting on the genome SRE to regulate gene expression (Oh et al., 2010). Our study suggests that DHA can regulate zebrafish *cyp11a1* promoter activity through a GPR120-like pathway in 293T cells and zebrafish embryos. Future investigations should aim to identify the GPR120-like receptor potentially mediating DHA ligand-receptor signaling in fish.

SUPPLEMENTARY DATA

Supplementary data to this article can be found online.

COMPETING INTERESTS

The authors declare that they have no competing interests.

AUTHORS' CONTRIBUTIONS

Y.H.S. conceived and designed the study and supervised the analyses. Y.L., X.H.L., D.Y., R.Z., and C.J.L. prepared the data. Y.L. and Y.H.S. analyzed the data. Y.L., M.D.H., and H.P.W. prepared the draft of the manuscript. W.H. provided resources. Y.L. and Y.H.S. revised and finalized the manuscript. All authors read and approved the final version of the manuscript.

REFERENCES

Agarwal A, Aponte-Mellado A, Premkumar BJ, et al. 2012. The effects of oxidative stress on female reproduction: a review. *Reproductive Biology and Endocrinology*, **10**: 49.

Akhmanova A, Steinmetz MO. 2015. Control of microtubule organization and dynamics: two ends in the limelight. *Nature Reviews Molecular Cell*

Biology, **16**(12): 711−726.

Arita M, Bianchini F, Aliberti J, et al. 2005. Stereochemical assignment, antiinflammatory properties, and receptor for the omega-3 lipid mediator resolvin E1. *Journal of Experimental Medicine*, **201**(5): 713−722.

Arita M, Ohira T, Sun YP, et al. 2007. Resolvin E1 selectively interacts with leukotriene B_4 receptor BLT1 and ChemR23 to regulate inflammation. *The Journal of Immunology*, **178**(6): 3912−3917.

Cerri RLA, Juchem SO, Chebel RC, et al. 2009. Effect of fat source differing in fatty acid profile on metabolic parameters, fertilization, and embryo quality in high-producing dairy cows. *Journal of Dairy Science*, **92**(4): 1520−1531.

Chiu YH, Karmon AE, Gaskins AJ, et al. 2018. Serum omega-3 fatty acids and treatment outcomes among women undergoing assisted reproduction. *Human Reproduction*, **33**(1): 156−165.

Gu L, Liu HL, Gu X, et al. 2015. Metabolic control of oocyte development: linking maternal nutrition and reproductive outcomes. *Cellular and Molecular Life Sciences*, **72**(2): 251−271.

Han LR, Yu J, Chen YY, et al. 2018. Immunomodulatory activity of docosahexenoic acid on RAW264.7 cells activation through GPR120-mediated signaling pathway. *Journal of Agricultural and Food Chemistry*, **66**(4): 926−934.

He MD, Jiao SB, Zhang R, et al. 2022. Translational control by maternal Nanog promotes oogenesis and early embryonic development. *Development*, **149**(24): dev201213.

He MD, Zhang R, Jiao SB, et al. 2020. Nanog safeguards early embryogenesis against global activation of maternal β-catenin activity by interfering with TCF factors. *PLoS Biology*, **18**(7): e3000561.

Hilgendorf KI, Johnson CT, Mezger A, et al. 2019. Omega-3 fatty acids activate ciliary FFAR4 to control adipogenesis. *Cell*, **179**(6): 1289−1305.e21.

Hirasawa A, Tsumaya K, Awaji T, et al. 2005. Free fatty acids regulate gut incretin glucagon-like peptide-1 secretion through GPR120. *Nature Medicine*, **11**(1): 90−94.

Hoo JY, Kumari Y, Shaikh MF, et al. 2016. Zebrafish: a versatile animal model for fertility research. *BioMed Research International*, **2016**: 9732780.

Hsu HJ, Hsu NC, Hu MC, et al. 2006a. Steroidogenesis in zebrafish and mouse models. *Molecular and Cellular Endocrinology*, **248**(1-2): 160−163.

Hsu HJ, Liang MR, Chen CT, et al. 2006b. Pregnenolone stabilizes microtubules and promotes zebrafish embryonic cell movement. *Nature*, **439**(7075): 480−483.

Hsu HJ, Lin JC, Chung BC. 2009. Zebrafish *cyp11a1* and *hsd3b* genes: structure, expression and steroidogenic development during embryogenesis. *Molecular and Cellular Endocrinology*, **312**(1-2): 31−34.

Hu MC, Hsu HJ, Guo IC, et al. 2004. Function of *Cyp11a1* in animal models. *Molecular and Cellular Endocrinology*, **215**(1-2): 95−100.

Janati Idrissi S, Slezec-Frick V, Le Bourhis D, et al. 2022. Effect of DHA on the quality of *in vitro* produced bovine embryos. *Theriogenology*, **187**: 102−111.

Jesuthasan S, Strähle U. 1997. Dynamic microtubules and specification of the zebrafish embryonic axis. *Current Biology*, **7**(1): 31−42.

Jiao SB, He MD, Sun YH. 2023. Research progress and several key scientific questions in studies of fish egg quality. *Acta Hydrobiologica Sinica*, **47**(6): 1007−1024. (in Chinese)

Katakura M, Hashimoto M, Shahdat HM, et al. 2009. Docosahexaenoic acid promotes neuronal differentiation by regulating basic helix-loop-helix transcription factors and cell cycle in neural stem cells. *Neuroscience*, **160**(3): 651−660.

Kniazeva M, Sieber M, McCauley S, et al. 2003. Suppression of the ELO-2 FA elongation activity results in alterations of the fatty acid composition and multiple physiological defects, including abnormal ultradian rhythms, in *Caenorhabditis elegans*. *Genetics*, **163**(1): 159–169.

Krisher RL. 2013. *In vivo* and *in vitro* environmental effects on mammalian oocyte quality. *Annual Review of Animal Biosciences*, **1**: 393−417.

Lauritzen L, Brambilla P, Mazzocchi A, et al. 2016. DHA effects in brain development and function. *Nutrients*, **8**(1): 6.

Li YY, Chen WZ, Sun ZW, et al. 2004. Effects of *n*-3 HUFA content in broodstock diets on reproductive performance and seasonal changes of plasma sex steroids levels in *Plectorhynchus cinctus*. *Zoological Research*, **25**(3): 249–255. (in Chinese)

Liu CJ, Ye D, Wang HP, et al. 2020. Elovl2 but not Elovl5 is essential for the biosynthesis of docosahexaenoic acid (DHA) in zebrafish: Insight from a comparative gene knockout study. *Marine Biotechnology*, **22**(5): 613−619.

Loehfelm A, Elder MK, Boucsein A, et al. 2020. Docosahexaenoic acid prevents palmitate induced insulin dependent impairments of neuronal health. *The FASEB Journal*, **34**(3): 4635−4652.

Lu FI, Sun YH, Wei CY, et al. 2014. Tissue specific derepression of TCF/LEF controls the activity of the Wnt/β-catenin pathway. *Nature Communications*, **5**: 5368.

MacRae CA, Peterson RT. 2015. Zebrafish as tools for drug discovery. *Nature Reviews Drug Discovery*, **14**(10): 721−731.

Maillard V, Desmarchais A, Durcin M, et al. 2018. Docosahexaenoic acid (DHA) effects on proliferation and steroidogenesis of bovine granulosa cells. *Reproductive Biology and Endocrinology*, **16**(1): 40.

Masoudi R, Sharafi M, Zare Shahneh A, et al. 2016. Effect of dietary fish oil supplementation on ram semen freeze ability and fertility using soybean lecithin-and egg yolk-based extenders. *Theriogenology*, **86**(6): 1583−1588.

Miao YL, Cui Z, Gao Q, et al. 2020. Nicotinamide mononucleotide supplementation reverses the declining quality of maternally aged oocytes. *Cell Reports* **32**(5): 107987.

Monroig O, Tocher DR, Castro LFC. 2018. Polyunsaturated fatty acid biosynthesis and metabolism in fish. *In*: Burdge GC. Polyunsaturated Fatty Acid Metabolism. Amsterdam: Elsevier, 31–60.

Muskiet FAJ, Fokkema MR, Schaafsma A, et al. 2004. Is Docosahexaenoic Acid (DHA) Essential? Lessons from DHA status regulation, our ancient diet, epidemiology and randomized controlled trials. *The Journal of Nutrition*, **134**(1): 183−186.

Nehra D, Le HD, Fallon EM, et al. 2012. Prolonging the female reproductive lifespan and improving egg quality with dietary omega-3 fatty acids. *Aging Cell*, **11**(6): 1046−1054.

Oh DY, Talukdar S, Bae EJ, et al. 2010. GPR120 is an omega-3 fatty acid receptor mediating potent anti-inflammatory and insulin-sensitizing effects. *Cell*, **142**(5): 687−698.

Ojeda SR, Naor Z, Negro-Vilar A. 1979. The role of prostaglandins in the control of gonadotropin and prolactin secretion. *Prostaglandins and Medicine*, **2**(4): 249−275.

Olsen SF, Halldorsson TI, Li M, et al. 2019. Examining the effect of fish oil supplementation in Chinese pregnant women on gestation duration and risk of preterm delivery. *The Journal of Nutrition*, **149**(11): 1942−1951.

Pang SC, Wang HP, Li KY, et al. 2014. Double transgenesis of humanized *fat1* and *fat2* genes promotes omega-3 polyunsaturated fatty acids synthesis in a zebrafish model. *Marine Biotechnology*, **16**(5): 580−593.

Pusceddu MM, Nolan YM, Green HF, et al. 2016. The omega-3 polyunsaturated fatty acid docosahexaenoic acid (DHA) reverses corticosterone-induced changes in cortical neurons. *International Journal of Neuropsychopharmacology*, **19**(6): pyv130.

Qi XL, Shang MY, Chen C, et al. 2019. Dietary supplementation with linseed oil improves semen quality, reproductive hormone, gene and protein expression related to testosterone synthesis in aging layer breeder roosters. *Theriogenology*, **131**: 9−15.

Serrano-García N, Fernández-Valverde F, Luis-Garcia ER, et al. 2018. Docosahexaenoic acid protection in a rotenone induced Parkinson's model: prevention of tubulin and synaptophysin loss, but no association with

mitochondrial function. *Neurochemistry International*, **121**: 26−37.
Shin JI, Jeon YJ, Lee S, et al. 2019. G-protein-coupled receptor 120 mediates DHA-induced apoptosis by regulating IP3R, ROS and, ER stress levels in cisplatin-resistant cancer cells. *Molecules and Cells*, **42**(3): 252−261.
Stoffel W, Holz B, Jenke B, et al. 2008. Δ6-desaturase (FADS2) deficiency unveils the role of ω3- and ω6-polyunsaturated fatty acids. *The EMBO Journal*, **27**(17): 2281−2292.
Sun QY, Lai LX, Park KW, et al. 2001. Dynamic events are differently mediated by microfilaments, microtubules, and mitogen-activated protein kinase during porcine oocyte maturation and fertilization in vitro. *Biology of Reproduction*, **64**(3): 879−889.
Swanson D, Block R, Mousa SA. 2012. Omega-3 fatty acids EPA and DHA: health benefits throughout life. *Advances in Nutrition*, **3**(1): 1−7.
Tocher DR. 2003. Metabolism and functions of lipids and fatty acids in teleost fish. *Reviews in Fisheries Science*, **11**(2): 107−184.
Tran DQ, Ramos EH, Belsham DD. 2016. Induction of *Gnrh* mRNA expression by the ω-3 polyunsaturated fatty acid docosahexaenoic acid and the saturated fatty acid palmitate in a GnRH-synthesizing neuronal cell model, mHypoA-GnRH/GFP. *Molecular and Cellular Endocrinology*, **426**: 125−135.
Tran LD, Hino H, Quach H, et al. 2012. Dynamic microtubules at the vegetal cortex predict the embryonic axis in zebrafish. *Development*, **139**(19): 3644−3652.
Vrablik TL, Watts JL. 2013. Polyunsaturated fatty acid derived signaling in reproduction and development: insights from *Caenorhabditis elegans* and *Drosophila melanogaster*. *Molecular Reproduction & Development*, **80**(4): 244–259.
Wang YQ, Ye D, Zhang FH, et al. 2022. *Cyp11a2* Is essential for oocyte development and spermatogonial stem cell differentiation in zebrafish. *Endocrinology*, **163**(2): bqab258.
Wang X, Zhu J, Wang H, et al. 2023. Induced formation of primordial germ cells from zebrafish blastomeres by germplasm factors. *Nature Communications*, **14**(1): 7918.
Wathes DC, Abayasekara DRE, Aitken RJ. 2007. Polyunsaturated fatty acids in male and female reproduction. *Biology of Reproduction*, **77**(2): 190−201.
Wei CY, Wang HP, Zhu ZY, et al. 2014. Transcriptional factors Smad1 and Smad9 act redundantly to mediate zebrafish ventral specification downstream of Smad5. *Journal of Biological Chemistry*, **289**(10): 6604−6618.
Weng JH, Liang MR, Chen CH, et al. 2013. Pregnenolone activates CLIP-170 to promote microtubule growth and cell migration. *Nature Chemical Biology*, **9**(10): 636−642.
Wonnacott KE, Kwong WY, Hughes J, et al. 2010. Dietary omega-3 and -6 polyunsaturated fatty acids affect the composition and development of sheep granulosa cells, oocytes and embryos. *Reproduction*, **139**(1): 57−69.
Xu HG, Cao L, Wei YL, et al. 2017. Effects of different dietary DHA: EPA ratios on gonadal steroidogenesis in the marine teleost, tongue sole (*Cynoglossus semilaevis*). *British Journal of Nutrition*, **118**(3): 179−188.
Xu SS, Li Y, Wang HP, et al. 2023. Depletion of *stearoyl-CoA desaturase* (*scd*) leads to fatty liver disease and defective mating behavior in zebrafish. *Zoological Research*, **44**(1): 63−77.
Yang YJ, Wang Y, Li Z, et al. 2017. Sequential, divergent, and cooperative requirements of *Foxl2a* and *Foxl2b* in ovary development and maintenance of zebrafish. *Genetics*, **205**(4): 1551−1572.
Ye D, Tu YX, Wang HP, et al. 2022. A landscape of differentiated biological processes involved in the initiation of sex differentiation in zebrafish. *Water Biology and Security*, **1**(3): 100059.
Ye D, Zhu L, Zhang QF, et al. 2019. Abundance of early embryonic primordial germ cells promotes zebrafish female differentiation as revealed by lifetime labeling of germline. *Marine Biotechnology*, **21**(2): 217−228.
Zadravec D, Tvrdik P, Guillou H, et al. 2011. ELOVL2 controls the level of n-6 28: 5 and 30: 5 fatty acids in testis, a prerequisite for male fertility and sperm maturation in mice. *Journal of Lipid Research*, **52**(2): 245−255.
Zeituni EM, Farber SA. 2016. Studying lipid metabolism and transport during zebrafish development. *In*: Kawakami K, Patton E, Orger M. Zebrafish: Methods and Protocols. New York: Humana Press, 237–255.
Zhang QF, Ye D, Wang HP, et al. 2020. Zebrafish *cyp11c1* knockout reveals the roles of 11-ketotestosterone and Cortisol in sexual development and reproduction. *Endocrinology*, **161**(6): bqaa048.
Zhang R, Tu YX, Ye D, et al. 2022. A germline-specific regulator of mitochondrial fusion is required for maintenance and differentiation of germline stem and progenitor cells. *Advanced Science*, **9**(36): 2203631.
Zhang TT, Xu J, Wang YM, et al. 2019a. Health benefits of dietary marine DHA/EPA-enriched glycerophospholipids. *Progress in Lipid Research*, **75**: 100997.
Zhang XF, Pang SC, Liu CJ, et al. 2019b. A novel dietary source of EPA and DHA: metabolic engineering of an important freshwater species-common carp by *fat1*-transgenesis. *Marine Biotechnology*, **21**(2): 171−185.
Zhou Q. 2013. Advances in the study of neuroendocrinological regulation of kisspeptin in fish reproduction. *Zoological Research*, **34**(5): 519−530.
Zhu YH, Tan QS, Zhang LS, et al. 2019. The migration of docosahexenoic acid (DHA) to the developing ovary of female zebrafish (*Danio rerio*). *Comparative Biochemistry and Physiology Part A:Molecular & Integrative Physiology*, **233**: 97−105.